




# A climate database with varying drought-heat signatures for climate impact modelling

Elisabeth Tschumi<sup>1,2</sup>  | Sebastian Lienert<sup>1,2</sup> | Karin van der Wiel<sup>3</sup> | Fortunat Joos<sup>1,2</sup> | Jakob Zscheischler<sup>1,2,4</sup>

<sup>1</sup>Climate and Environmental Physics, University of Bern, Bern, Switzerland

<sup>2</sup>Oeschger Centre for Climate Change Research, University of Bern, Bern, Switzerland

<sup>3</sup>Royal Netherlands Meteorological Institute, De Bilt, The Netherlands

<sup>4</sup>Department of Computational Hydrosystems, Helmholtz Centre for Environmental Research – UFZ, Leipzig, Germany

## Correspondence

Elisabeth Tschumi, Climate and Environmental Physics, University of Bern, Bern, Switzerland.  
Email: elisabeth.tschumi@climate.unibe.ch

## Funding information

E.T. and J.Z. acknowledge the Swiss National Science Foundation (Ambizione grant 179876). J.Z. further acknowledges the Helmholtz Initiative and Networking Fund (Young Investigator Group COMPOUNDX, Grant Agreement VH-NG-1537). K.v.d.W. acknowledges funding for the HiWAVES3 project from the National Natural Science Foundation of China (41661144006), funding was supplied through JPI Climate and the Belmont Forum (NWO ALWCL.2.016.2 and NSFC 41661144006). F.J. and S.L. acknowledge funding from the Swiss National Science Foundation (Grant no.

## Abstract

Extreme climate events, such as droughts and heatwaves, can have large impacts on the environment. Disentangling their individual and combined effects is a difficult task, due to the challenges associated with generating controlled environments to study differences in their impacts. One approach to this problem is creating artificial climate forcing with varying magnitude of univariate and compound extremes, which can be applied to process-based impact models. Here, we propose and describe a set of six 100-year long climate scenarios with varying drought-heat signatures that are derived from climate model simulations whose mean climate is comparable to present-day climate conditions. The changes in extremes are most notable in the 3 months in which vegetation activity is highest and where arguably hot and dry extremes may have the largest impacts. Besides a control scenario representing natural variability (Control), one scenario has neither heat nor drought extremes (Noextremes), one has univariate extremes but no compound extremes (Nocompound), one has only heat extremes but few droughts (Hot), one has only droughts but few heatwaves (Dry),

## Dataset

Identifier: <https://doi.org/10.5281/zenodo.4385445>

Creators: Elisabeth Tschumi, Sebastian Lienert, Karin van der Wiel, Fortunat Joos, Jakob Zscheischler

Dataset correspondence: elisabeth.tschumi@climate.unibe.ch

Title: A climate database with varying drought-heat signatures for climate impact modelling

Publisher: Zenodo

Publication year: 2020

Resource type: Dataset

Version: version1.0

Conflict of interests: The authors declare that they have no competing interests.

This is an open access article under the terms of the Creative Commons Attribution License, which permits use, distribution and reproduction in any medium, provided the original work is properly cited.

© 2021 The Authors. *Geoscience Data Journal* published by Royal Meteorological Society and John Wiley & Sons Ltd.

172476) and from the European Union's Horizon 2020 Research and Innovation Programme under grant agreement no. 821003 (project 4C, Climate-Carbon Interactions in the Current Century). The work reflects only the authors' view; the European Commission and their executive agency are not responsible for any use that may be made of the information the work contains

and one has many compound heat and drought extremes (Hotdry). These scenarios differ only moderately in their global mean climate (about 0.3°C in temperature and 6% in precipitation) and do not contain any long-term trends. The data are provided on a daily timescale over land (except Antarctica and parts of Greenland) on a regular 1° × 1° grid. These scenarios were constructed primarily to investigate the impact of varying drought-heat signatures on vegetation and the terrestrial carbon cycle. However, we believe that they may also prove useful to study the differential impacts of droughts and heatwaves in other areas, such as the occurrence of wildfires or crop failure. The data described here can be found on zenodo (<https://doi.org/10.5281/zenodo.4385445>, Tschumi et al., 2020).

#### KEYWORDS

climate model data, compound events, droughts, extremes, heatwaves

## 1 | INTRODUCTION

Climate extremes such as droughts, heatwaves, storms and floods are important stressors to the natural environment. They can lead to large and devastating impacts on ecosystems and society (Frank et al., 2015; IPCC, 2012; Reichstein et al., 2013; Tschumi & Zscheischler, 2020). Extreme impacts, in turn, may also be caused by meteorological conditions that are not necessarily extreme in a statistical sense (Van der Wiel et al., 2020; Vogel et al., 2021; Zscheischler et al., 2016). In many cases, impacts are caused by multiple extremes or a combination of anomalous meteorological drivers (Flach et al., 2017), also referred to as compound events (Zscheischler et al., 2018, 2020). The multiple drivers behind compound events are often correlated (Leonard et al., 2014; Zscheischler & Seneviratne, 2017). Furthermore, the combined impact of compound extremes can be more severe than a simple linear combination of univariate extremes, for instance, the effect of drought and heat on terrestrial carbon uptake (Zscheischler et al., 2014b) or crop yields (Cohen et al., 2020; Ribeiro et al., 2020). Hence, quantifying the differential impact of compound versus univariate extremes and the relevance of driver dependence is important for a better understanding of climate risks.

The land biosphere plays an important role in the global carbon cycle, taking up between a quarter and a third of anthropogenic CO<sub>2</sub> emissions (31% in the last decade according to the most recent estimate of the Global Carbon Project, Friedlingstein et al., 2020). Different factors enhance this land sink such as increased atmospheric CO<sub>2</sub> concentrations and warmer temperatures in the high latitudes, which increase the growing season length in the high latitudes (Zhu et al., 2016). However, at the local scale, vegetation productivity can be limited by factors such as water availability, temperature conditions, light conditions, availability of nutrients and

CO<sub>2</sub> concentrations (Schlesinger & Bernhard, 2013). These factors can vary greatly, especially during extreme climate conditions.

The effect of climate extremes on vegetation and the terrestrial carbon cycle can be studied from different perspectives, for instance based on (a) lab or field experiments (Beier et al., 2012; De Boeck et al., 2011; Song et al., 2019), (b) observational data such as long-term forest observations (Anderegg et al., 2013) and local measurements of carbon exchange (Ciais et al., 2005; Pastorello et al., 2020; von Buttlar et al., 2018), (c) indirect estimates from satellite observations (Ciais et al., 2005; Stocker et al., 2019; Zhao & Running, 2010; Zscheischler et al., 2013) and (d) dynamical vegetation models (Bastos et al., 2020; Ciais et al., 2005; Pan et al., 2020; Rammig et al., 2015; Xu et al., 2019; Zscheischler et al., 2014a, 2014b, 2014c, 2014d). Hereby, process-based vegetation models allow for the development and testing of novel hypotheses in a controlled environment and at the global scale. Arguably, drought and heat are amongst the most damaging hazards to terrestrial vegetation (Allen et al., 2010; Frank et al., 2015; Reichstein et al., 2013; Sippel et al., 2018; Zscheischler et al., 2014b). However, differentiating impacts between drought and heat alone and compound drought and heat remains a challenging task. Despite the large model uncertainties, it is widely acknowledged that drought and heat extremes will increase in frequency and severity in many land regions in the future (Seneviratne et al., 2012). Though it is still uncertain exactly how these increases will affect the terrestrial biosphere, there are concerns they might substantially reduce the current terrestrial carbon sink (Reichstein et al., 2013).

Temperature and precipitation are strongly correlated in most land regions in the warm season (Madden & Williams, 1978; Trenberth & Shea, 2005), and this dependence controls the occurrence of compound drought and heatwave events

(Zscheischler & Seneviratne, 2017). Similar to regional biases in mean temperature and precipitation, climate models can have biases in the temperature-precipitation dependence, that is, in the correlation between temperature and precipitation. Given the relevance of drought and heat for carbon dynamics and, in particular, the disproportional impacts of compound drought and heat (Allen et al., 2010; von Buttlar et al., 2018; Zscheischler et al., 2014d), differences in the dependence between temperature and precipitation in the climate forcing might affect estimates of carbon dynamics and uptake. In particular, Earth system models collected in the coupled model intercomparison projects (e.g. CMIP5 Taylor et al., 2012) show a substantially stronger dependence than the forcing that is used in the regular carbon budget estimates provided by the Global Carbon Project (Friedlingstein et al., 2020) in the Southern Hemisphere (Zscheischler & Seneviratne, 2017). It is unclear whether these differences originate from an overestimation of the dependence in climate models or a lack of observational constraint in observation-based gridded climate datasets. However, independent of a potential bias with respect to observations, differences in this dependence across climate models may contribute to uncertainties in carbon-cycle climate feedbacks with ongoing climate change (Friedlingstein et al., 2014).

Disentangling the effects of varying temperature-precipitation dependence and the associated occurrence of compound drought and heat on terrestrial carbon dynamics is challenging, as non-stationarity and the use of different vegetation models in different Earth system models confound the assessment. Here, we present a range of climate scenarios that have been developed specifically to study the differential effects of single or compound drought and heat events and their impacts on vegetation and the terrestrial carbon cycle with dynamical vegetation models. The scenarios span a period of 100 years, and all have a similar mean climate but differ in their occurrence frequency and intensity of droughts, heatwaves and compound drought and heatwave events during the peak of the growing season. Although the scenarios are somewhat tailored to study carbon dynamics, they may also be used to explore the effects of drought and heat on other climate impacts, for example, wildfires or crop failure.

## 2 | DATA DESCRIPTION

This section describes the climate model simulations from that the scenarios were sampled. We further provide an assessment of biases in precipitation and temperature and show that our climate simulations with approximately constant forcing result in a stationary vegetation composition over time. Finally, we describe how we sampled scenarios with different drought-heat signatures.

### 2.1 | EC-Earth climate simulations

The data for the drought-heat scenarios were sampled from a large ensemble climate modelling experiment. This experiment consisted of 2000 years of simulated present-day climate data, which were created with the fully coupled global climate model EC-Earth (v2.3, Hazeleger et al., 2012). The large ensemble was built out of 400 short five-year runs, which were unique in initial condition and/or stochastic physics seed. EC-Earth combines atmospheric, oceanic, land and sea-ice model components and simulates the global climate including feedbacks between, for example, land and atmosphere. The horizontal resolution in the atmosphere for the simulations was T159 (approximately  $1.1^\circ$ ). For creating the scenarios, the climate model output has been bilinearly interpolated to a regular  $1^\circ \times 1^\circ$  grid. All analysis was based on daily data.

In the large ensemble experiment, we defined the ‘present-day climate’ by means of the observed global mean surface temperature over the years 2011–2015. We selected the five year EC-Earth model period (2035–2039) that minimized the difference between simulations and observation of the global mean surface temperature from 16 transient climate runs (1861–2100, RCP8.5). Each of these 16 runs were then used, at the start of the selected period, as an initial condition for an ensemble of 25 members of 5 years each. By choosing different seeds for the atmospheric stochastic perturbations (Buizza et al., 1999), each of these members developed unique weather. Together this resulted in  $16 \times 25 \times 5 = 2000$  years of simulated present-day climate data. More details on the large ensemble climate model experiment setup are provided in Van der Wiel et al. (2019c). Note that, within the ensemble, the influence of forced climate change is small. We, therefore, assume that all variability in the dataset is due to natural variability in the climate system.

### 2.2 | Regional biases in annual temperature and precipitation

Despite the annual mean surface temperature being unbiased at the global scale by experimental design (Section 2.1), model biases may exist at the regional and seasonal scale. We, therefore, compare a random 100 year sample from the EC-Earth data to a 30-year climatology of the climate data from the Climate Research Unit (CRU TS3.26) (Harris et al., 2014). We compared against the time period 1988–2017, though using a shorter time period of 2011–2015 (the same time period as represented by EC-Earth) results in very similar biases. Generally, averaged over land (excluding Antarctica and most of Greenland), temperature differs by  $-0.5^\circ\text{C}$  and precipitation by 7% compared to CRU. However, biases can be relatively large at the regional scale. In the tropics

(between 23.5°S and 23.5°N), EC-Earth has a cold bias of  $-1.8^{\circ}\text{C}$  compared to CRU (Figure 1a). In the extratropics, EC-Earth has a small warm bias of about  $0.2^{\circ}\text{C}$  on average, with most of this bias being concentrated in the very high latitudes and nearly no bias in the mid-latitudes (Figure 1a). With respect to annual precipitation, many land regions have a wet bias in EC-Earth compared to CRU (Figure 1b). The extratropics have a wet bias of about 43.5%. In the tropics, some regions are drier (e.g. the Amazon and Indonesia) whilst others have very little bias in EC-Earth compared to CRU (tropical Africa). Note, however, that observation-based estimates differ strongly in their absolute precipitation amounts (Sun et al., 2018).

### 2.3 | LPX-Bern stability

LPX-Bern v1.4 (Lienert & Joos, 2018) is a Dynamic Global Vegetation Model (DGVM) based on Lund-Potsdam-Jena (LPJ) model (Sitch et al., 2008). The model features coupled water, nitrogen and carbon cycles and represents different types of vegetation using Plant Functional Types (PFTs). Here, only natural vegetation is considered, which is internally represented by eight tree PFTs and two herbaceous PFTs competing for resources and adhering to bioclimatic limits. In this study, daily temperature, precipitation and short-wave radiation are provided to the model. Additionally, the model uses information on the soil type (Wieder et al., 2014),  $\text{CO}_2$  concentration in the atmosphere at 1901 level (296.8 ppm), and nitrogen deposition (NMIP; Tian et al., 2018). A spin-up of 1,500 years (recycling the first 30 years of the climate forcing) was performed to make sure all carbon pools are in equilibrium.

To make sure that the climate forcing is appropriate for climate impact modelling, we assessed whether LPX-Bern simulations are stable over the course of the entire 2,000 years of EC-Earth data. Except for a slight decreasing trend in tropical broadleaved evergreen trees (TrBE), the global fraction of each of the 10 PFTs present in LPX-Bern shows no apparent

trends over the 2,000 years (Figure S1). Hence, despite the relatively large biases at the regional scale (Section 2.2), LPX-Bern seems to be stable using input from this global climate model. This gives us confidence to use this control simulation as a baseline to estimate the effect of climate scenarios with different drought-heat signatures. We can assume that any trends and non-stationarities in the LPX-Bern output will be due to the scenarios. In addition, this test run was used for the sampling described in Section 2.4.

### 2.4 | Scenario sampling

This section describes the steps taken to create climate scenarios with varying drought-heat signatures. We sampled 100-year long scenarios from the original 2,000 years of EC-Earth data. The selection of the different scenarios was based on temperature and precipitation values during the time of the year where the vegetation is most active. Arguably, the vegetation is most vulnerable to climate extremes during the growing season (Orth et al., 2016; Zscheischler et al., 2017). Therefore, for the scenario creation we focused on the 3 months around the most productive month in the climatology. We first identified the most productive month at each pixel, that is, the month with the highest net primary production (NPP) in the mean seasonal cycle of NPP, as simulated by LPX-Bern (Section 2.3). The month of maximum NPP differs from pixel to pixel, depending on the geographical location (Figure S2). For instance, in the northern mid and high latitudes, July is typically the most productive month, whereas it is January or February in most of the southern mid and high latitudes. In contrast, in the tropics and subtropics, the most productive month varies quite strongly across locations, depending on the dominant rainy season (Wang & Ding, 2008).

We selected the six different scenarios for each pixel separately based on mean temperature and precipitation over the 3 months around the month of highest vegetation productivity: *Control*, *Noextremes*, *Nocompound*, *Hot*, *Dry* and

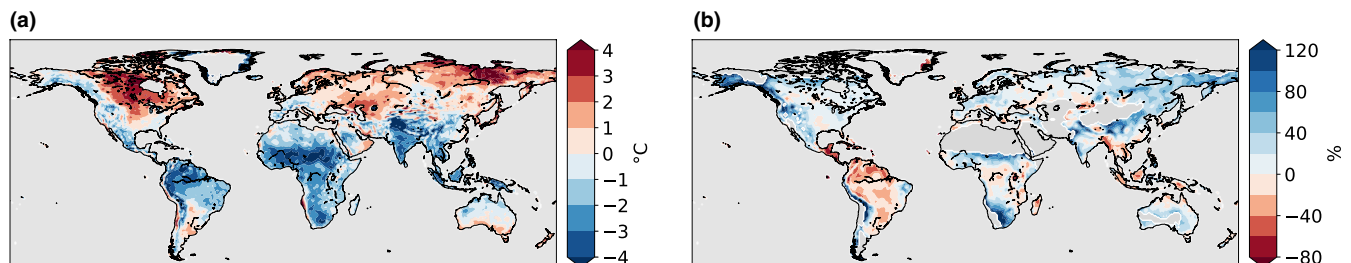


**FIGURE 1** Biases in EC-Earth simulations with respect to observation-based data from CRU. (a) Difference in annual mean temperature between EC-Earth and CRU in  $^{\circ}\text{C}$ . (b) Relative difference in annual precipitation between EC-Earth and CRU in %. The time period 1988–2017 was used for CRU and randomly sampled 100 years (representing 2011–2015) for EC-Earth. The land regions depicted in grey in (b) are desert regions with a mean annual precipitation of less than 250 mm in the CRU dataset and were excluded in the maps to avoid dividing by very small numbers

*Hotdry*. Years contributing to the scenarios were sampled based on quantiles of the 3 month temperature and precipitation averages as indicated in Figure 2, where the quantiles were computed based on the full 2,000-year EC-Earth simulation. If more than the required number of years fall into the quantiles in question, a random selection was performed. If less years than necessary were available, some randomly chosen years were selected multiple times.

- For Control, 100 years were sampled randomly out of the 2,000 years (Figure 2a).
- For Noextremes, 100 years were sampled for which temperature and precipitation are both within the 40th to 60th percentile (Figure 2b).
- For Nocompound, 100 years were sampled for which temperature and precipitation do not exceed the 85th percentile in any direction at the same time (Figure 2c).
- For Hot, 50 years were sampled for which temperature exceeds the 85th percentile and precipitation is within the 40th to 60th percentile and 50 years were sampled randomly from the rest (Figure 2d).
- For Dry, 50 years were sampled for which precipitation lies below the 15th percentile and temperature is within the 40th to 60th percentile and 50 years were sampled randomly from the rest (Figure 2e).
- For Hotdry, 50 years were sampled for which temperature lies above the 85th percentile and precipitation lies below the 15th percentile at the same time and 50 years were sampled randomly from the rest (Figure 2f).

The reason for only selecting 50 years from the extreme quantile for the Hot, Dry and Hotdry scenarios is twofold. Firstly, for many pixels, not a huge amount of years fall into the extreme quantiles. Sampling only 50 years from there reduces the numbers of times a year is resampled. Secondly, the mean climatology is kept more similar to the other scenarios if only half the years were sampled with extreme conditions and the other half from the rest.

This method of scenario creation, for each pixel separately, destroys any spatial coherence, so that the climate in a pixel is not correlated to the climate in nearby pixels. Furthermore, due to the sampling of individual years, there are always slight discontinuities between 31 December and 1 January in the climate forcing. The same is true for leap years, since all leap days (29 February) were removed.

## 2.5 | Available variables

To allow for impact modelling for a wide range of sectors, we provide temperature variables (mean, minimum, maximum), precipitation, radiation (short- and longwave downward

radiation and shortwave net radiation) and wind (zonal [eastward,  $u$ ] and meridional [northward,  $v$ ], see Table 1) at daily timescales. For this study, we only analysed mean temperature and precipitation to quantify differences in the occurrence of droughts and heatwaves between the scenarios. All variables are available at a regular  $1^\circ \times 1^\circ$  grid over land, except Antarctica and large parts of Greenland. Leap days were removed, so there are  $365 \times 100$  time steps for each scenario. Whenever global means are given, they are area-weighted means over all land cells except Antarctica and Greenland. The data can be accessed via zenodo (<https://doi.org/10.5281/zenodo.4385445>, Tschumi et al., 2020).

## 3 | SCENARIO CHARACTERIZATION

A key goal of the design of the different scenarios is that they vary in their characteristics of climate extremes, in particular droughts and heatwaves, whilst differing only little in their mean climate conditions. The scenarios differ moderately in their global land-mean temperature and annual precipitation sums and all scatter closely around global CRU averages (Figure 3). Temperature differences are in the order of  $0.3^\circ\text{C}$  and precipitation differences are up to 6%, which corresponds to about one and two standard deviations of the inter-annual variability in CRU, respectively. The precipitation differences between scenarios and with respect to CRU are thus noticeably smaller than the difference across different precipitation datasets (Sun et al., 2018). Spatially, explicit differences illustrate that the difference in annual mean temperature is mostly below  $1^\circ\text{C}$  for the Hot and Hotdry scenario at the regional scale, and much smaller for the other scenarios (Figure S3). Similarly, the difference in annual precipitation at the regional scale is mostly below 20% for the Hot, Dry and Hotdry scenario and much smaller for the others (Figure S4).

### 3.1 | Heatwaves

Temperature extremes were quantified based on cooling degree days (CDD). Being aware of the multitude of heatwave indices (Perkins, 2015), we chose this index because it is an integrative measure for cumulative magnitude, frequency and duration of the heatwaves (Lauferkötter et al., 2020). Choosing another index would result in different numbers but likely not affect the ranking between the different scenarios. Heating and cooling degree days are generally used in the energy sector to determine the energy needed to heat or cool a building, which is directly proportional to the number of heating or cooling degree days. Here, we calculated CDD as the sum of all temperature exceedances over a high threshold, in this

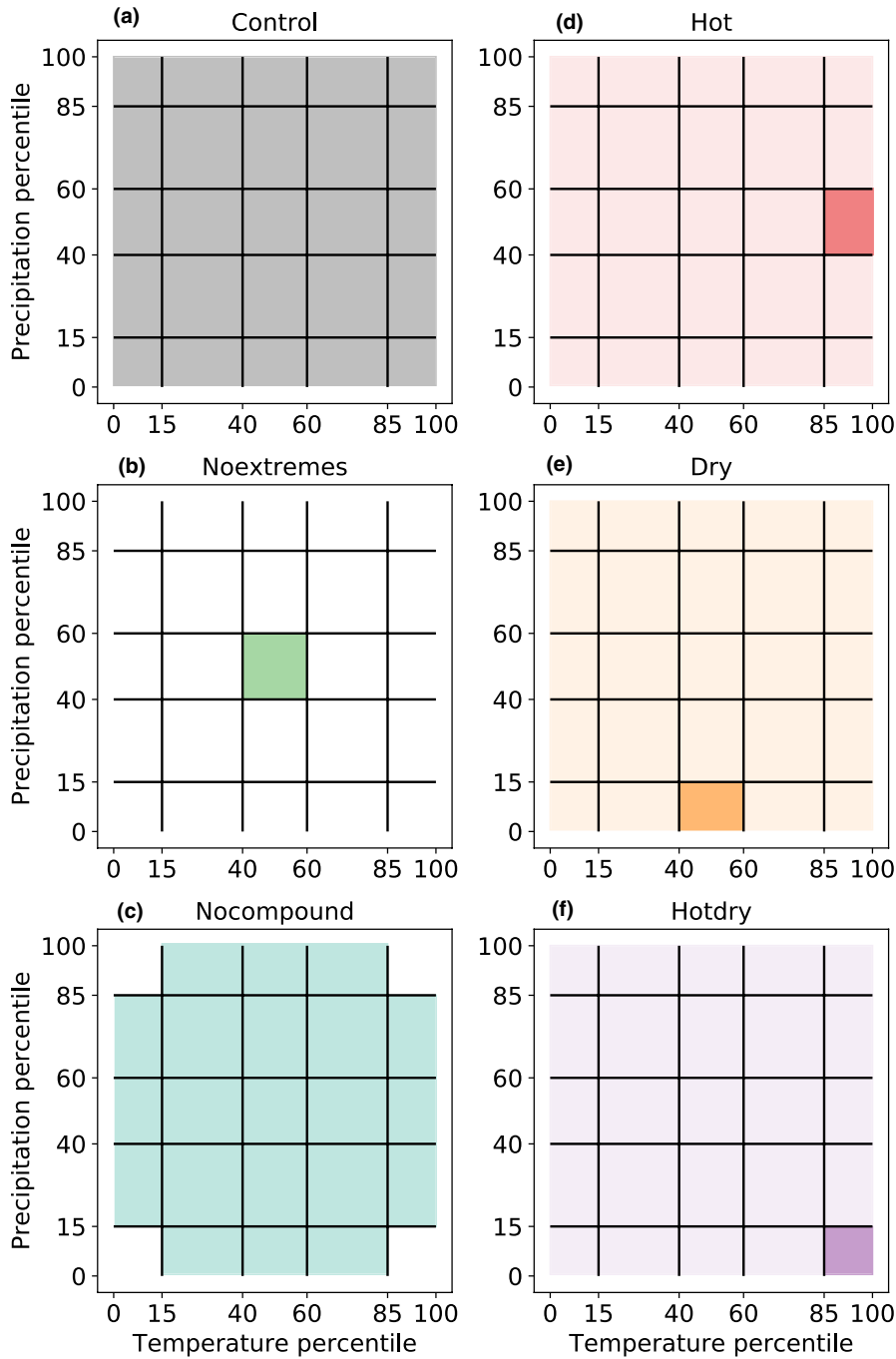


**FIGURE 2** Sampling of scenarios from their respective quantiles, details provided in the main text. Two colouring shades (for Hotdry, Hot and Dry) means 50 years were sampled from each shade. The quantiles were calculated based on the full 2,000 years EC-Earth data

case, the 90th percentile of the control scenario at each pixel, using daily temperature data:

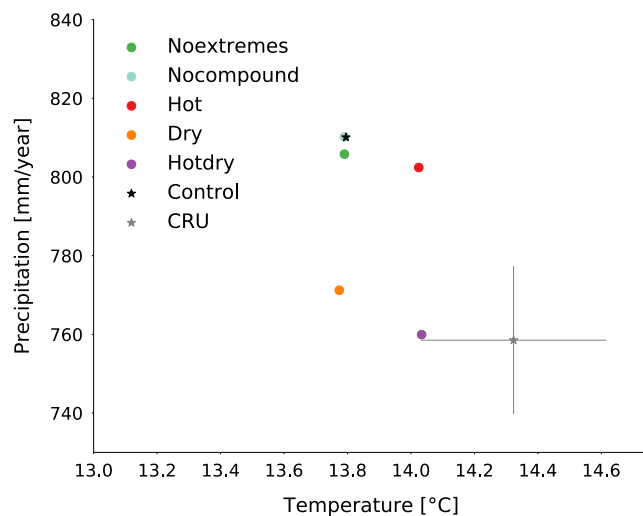
$$\text{CDD} = \sum_{i=1}^N (T_i - T_{90}) I_{T_i > T_{90}}. \quad (1)$$

Here,  $i$  indicates daily time steps,  $N$  is the total number of time steps ( $100 \times 365 = 36,500$  days),  $T_{90}$  denotes the 90th percentile of the local temperature time series and  $I$  denotes the indicator function, which is 1 if  $T_i > T_{90}$  and 0 otherwise.

In the Control scenario, CDD varies between close to zero and about  $100^\circ\text{C}$  per year, with higher numbers for regions further away from the equator, which can be explained by the higher temperature variability in extratropical regions compared to the tropics (Figure 4a). The Noextremes (global area-weighted mean relative difference between Noextremes and Control: 0.06%), Nocompound (global mean difference 6.9%) and Dry (global mean difference 4.7%) scenarios are very close to the Control in terms of CDD (Figure 4b,c,e). In contrast, in the Hot (global mean difference 42.7%) and Hotdry (global mean difference 47.9%) scenarios the CDDs

**TABLE 1** Available variables with a daily time step over land (except Antarctica and large parts of Greenland) on a  $1^\circ \times 1^\circ$  grid

Variable	Variable name	Unit	Description
Mean temperature	tas	$^\circ\text{C}$	Mean daily near-surface (2 m) temperature
Minimum temperature	tasmin	$^\circ\text{C}$	Minimum daily near-surface (2 m) temperature
Maximum temperature	tasmax	$^\circ\text{C}$	Maximum daily near-surface (2 m) temperature
Precipitation	pr	mm/day	Daily precipitation
Shortwave net radiation	sw	$\text{J day}^{-1} \text{m}^{-2}$	Shortwave net radiation
Shortwave downward radiation	swd	$\text{J day}^{-1} \text{m}^{-2}$	Shortwave downward radiation
Longwave downward radiation	lwd	$\text{J day}^{-1} \text{m}^{-2}$	Longwave downward radiation
Zonal wind	uas	m/s	Near-surface (10 m) eastward wind
Meridional wind	vas	m/s	Near-surface (10 m) northward wind

**FIGURE 3** Global annual average temperature and precipitation over land (excluding Antarctica and much of Greenland) for all scenarios and CRU (1988–2017). The bars on CRU indicate one standard deviation of annual means over the entire time period

increase by up to 160%, with the increases being slightly larger in the Hotdry scenario.

### 3.2 | Droughts

For the quantification of droughts we rely on the Standardized Precipitation Index (SPI) (McKee et al., 1993), one of the most widely used drought indicators. We use a three-month timescale based on monthly precipitation values and calculate SPI with the R package SPEI (Vicente-Serrano et al., 2010). The SPI is computed by fitting the three-month running mean monthly precipitation data to a Gamma distribution for each calendar month. The fitted Gamma distribution is then transformed to a standard normal distribution (McKee

et al., 1993). We investigate how the scenarios differ in their occurrence likelihood of severe droughts, defined as  $\text{SPI} < -1.5$ . Given that SPI is standard normally distributed, the occurrence probability of severe droughts is about 6.7%, which is captured well by most locations in the Control, except in the Sahara desert (Figure 5a). There is a slight reduction in number of severe droughts for the Noextremes scenario of  $-22.5\%$  in the global mean (Figure 5b), whereas the Nocompound ( $-4.7\%$ ) and the Hot ( $3.4\%$ ) scenario are fairly similar to the control (Figure 5c,d). The Dry ( $54.1\%$ ) and Hotdry ( $89.2\%$ ) scenario show large and very large increases in severe drought occurrence, up to 200% with respect to the control (Figure 5e,f). We repeated the drought analysis using the Standardized Precipitation-Evapotranspiration Index (SPEI) (Vicente-Serrano et al., 2010) instead of SPI. The SPEI also takes the effects of evapotranspiration into account and thus requires precipitation as well as temperature for its calculation (calculated here with the Hargreaves function based on monthly minimum/maximum temperature and precipitation; Vicente-Serrano et al., 2010). The spatial patterns are similar overall, though the changes are larger in particular for the Hotdry scenario (Figure S5).

### 3.3 | Compound extremes

Temperature and precipitation are negatively correlated during the most productive months in most regions of the world with a global mean Pearson correlation coefficient of  $-0.47$  in the control scenario (Figure 6). This inter-annual correlation was calculated using the vegetation periods most productive 3-month mean value per year for temperature and precipitation (the same 3 months that were used for the sampling). In contrast, in the Noextremes scenario, temperature and precipitation are hardly correlated at all (global mean  $-0.02$ ). The Nocompound ( $-0.31$ ), Hot ( $-0.37$ ), and Dry ( $-0.34$ )

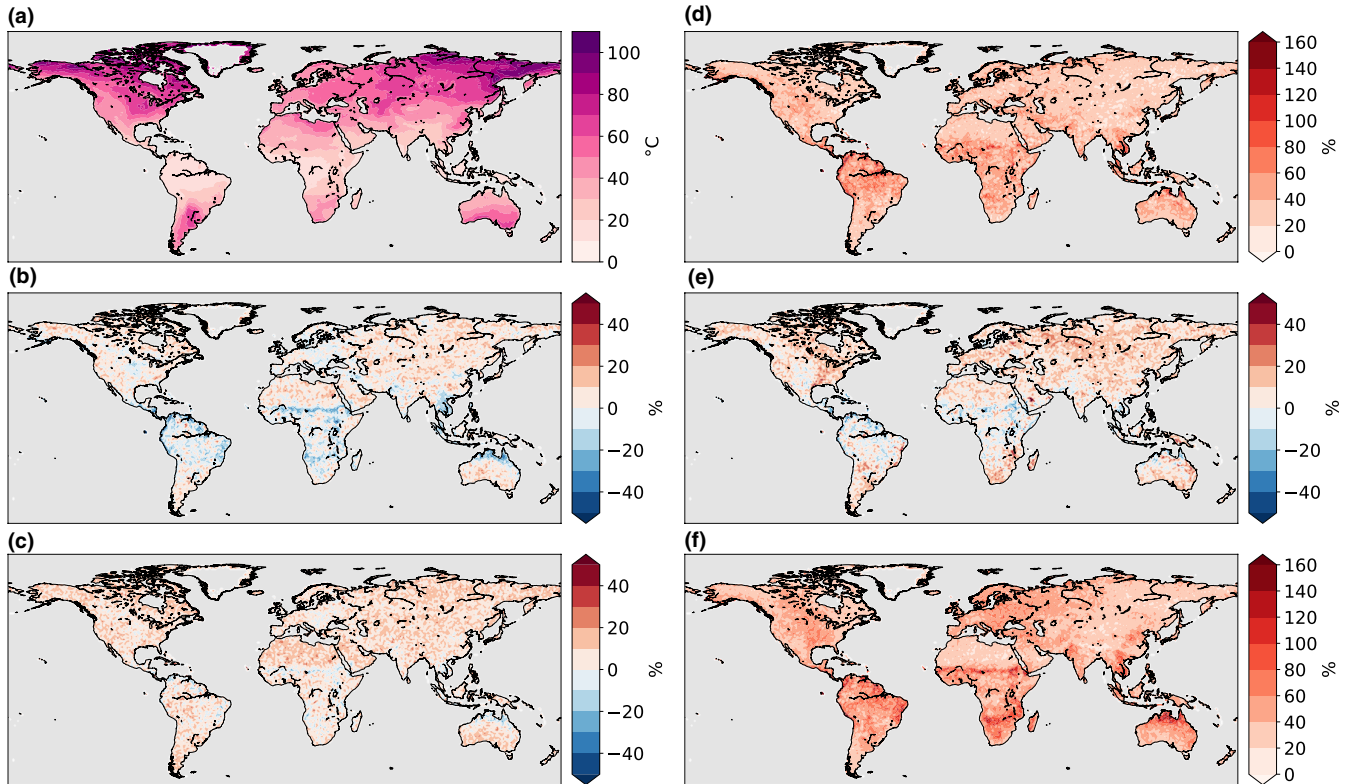


**FIGURE 4** Cooling Degree Days (CDD, normalized per year) as a metric for temperature extremes. (a) CDD in the Control scenario in °C. (b–f) Relative difference in CDD with respect to the Control scenarios in % (Noextremes (b), Nocompound (c), Hot (d), Dry (e) and Hotdry (f)). Note the different colour scales

scenarios all show a negative correlation between temperature and precipitation, but slightly less so compared to the control. The Hotdry scenario is the only scenario that features a strongly increased negative correlation between temperature and precipitation, with a global average of  $-0.72$ .

To measure the occurrence of compound hot and dry conditions, we assess the occurrence of compound hot and dry years. To this end, we calculate the frequency  $F$  of years for which the 3-month temperature lies above the 90th percentile and the 3-month precipitation lies below the 10th percentile of the control scenario.

$$F = \sum_{i=1}^{100} I_{T_i > T_{90}} I_{P_i < P_{10}} / 100. \quad (2)$$

In this equation (unlike Equation 1)  $i$  denotes a yearly time steps, ranging from 1 to the total number of years, that is, 100. If temperature and precipitation were completely independent, we would expect one out of 100 years to be a compound extreme year ( $F = 10\% \times 10\% = 1$ ). However, since they are strongly correlated over most land regions (Figure 6a) the global mean of compound hot and dry years for the control scenario is 3.6 years (Figure 7a). We further investigate probability ratios of compound extreme occurrence between scenarios and Control. Numbers smaller than

one mean fewer years with compound extremes than in the Control and vice versa. The Noextremes scenario contains no years with compound extremes (Figure 7b), and there are very few in the Nocompound scenario (probability ratio of 0.03, Figure 7c). In the global mean, Hot (0.65, Figure 7d) and Dry (0.66, Figure 7e) have a slight reduction of the number of years with compound extremes compared to Control. The Hotdry scenario shows a large increase in the occurrence of compound hot and dry years, with a probability ratio of 11.23 in the global average (Figure 7f). This shows that our scenario selection method, aimed to either remove or increase compound event occurrence, has been successful.

## 4 | DISCUSSION AND CONCLUSIONS

Disentangling the effects of single and compound drivers of climate impacts is challenging due to the difficulty to create a controlled environment, the representativity of local climate change experiments and many confounding factors related to non-stationarities in the climate system. One approach that allows to overcome most of these challenges is the use of climate models in combination with process-based impact models. Climate models allow for generating climate conditions without long-term trends that are representative



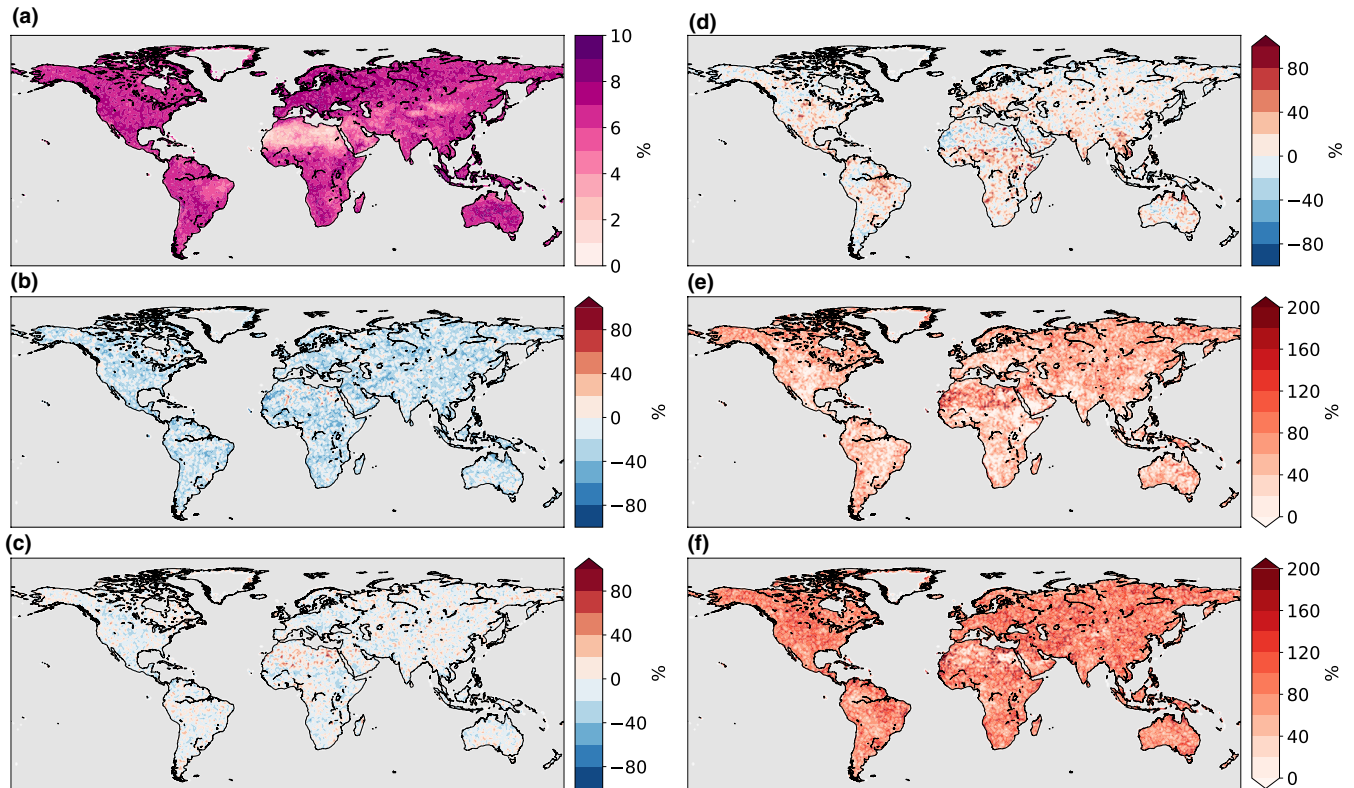


**FIGURE 5** Severe droughts. (a) Occurrence probability of severe droughts ( $SPI < -1.5$ ) in the Control scenario. (b–f) Relative difference in the percentage of severe droughts with respect to the Control scenario in % (Noextremes (b), Nocompound (c), Hot (d), Dry (e) and Hotdry (f)). Note the different colour scales

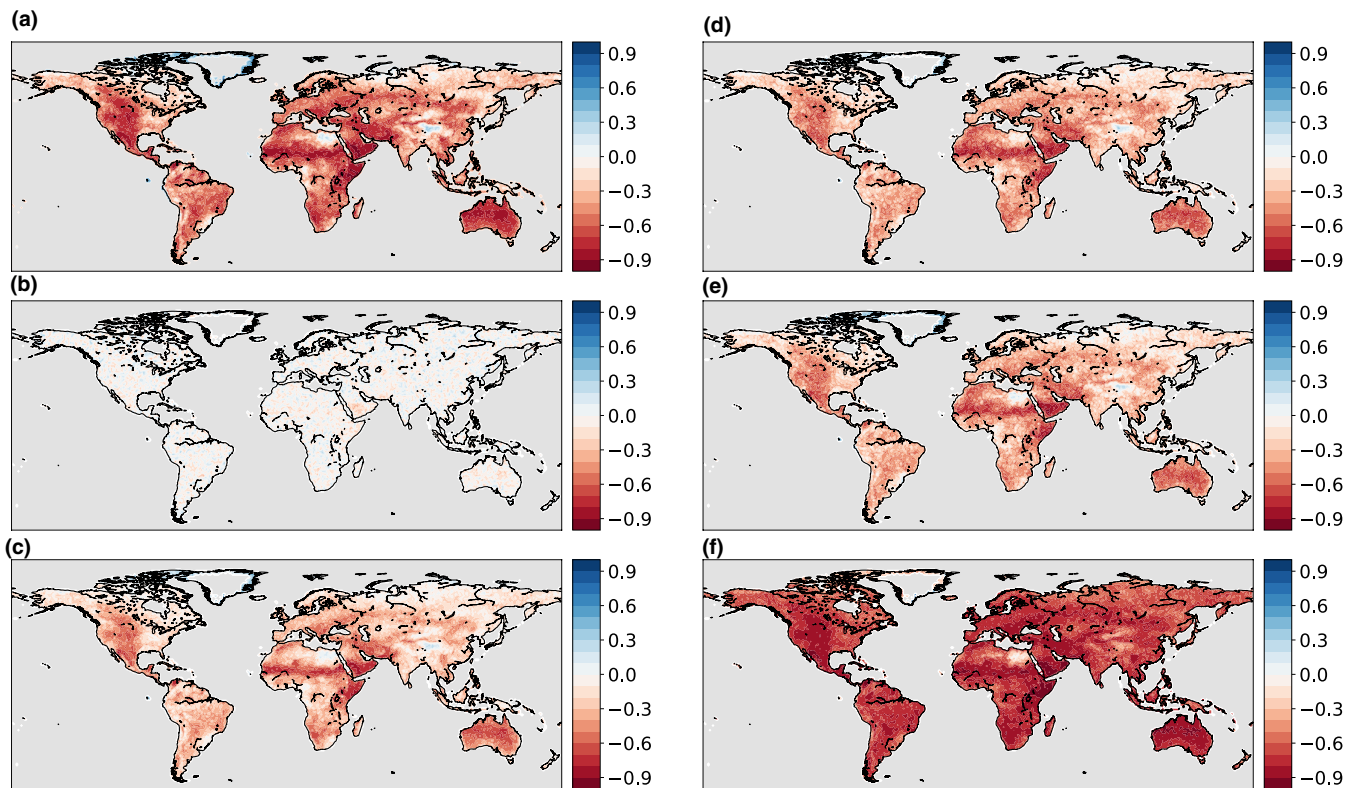


**FIGURE 6** Inter-annual correlation between temperature and precipitation during the 3 months when vegetation is most active. (a–f) The correlations between temperature and precipitation for Control (a), Noextremes (b), Nocompound (c), Hot (d), Dry (e) and Hotdry (f)

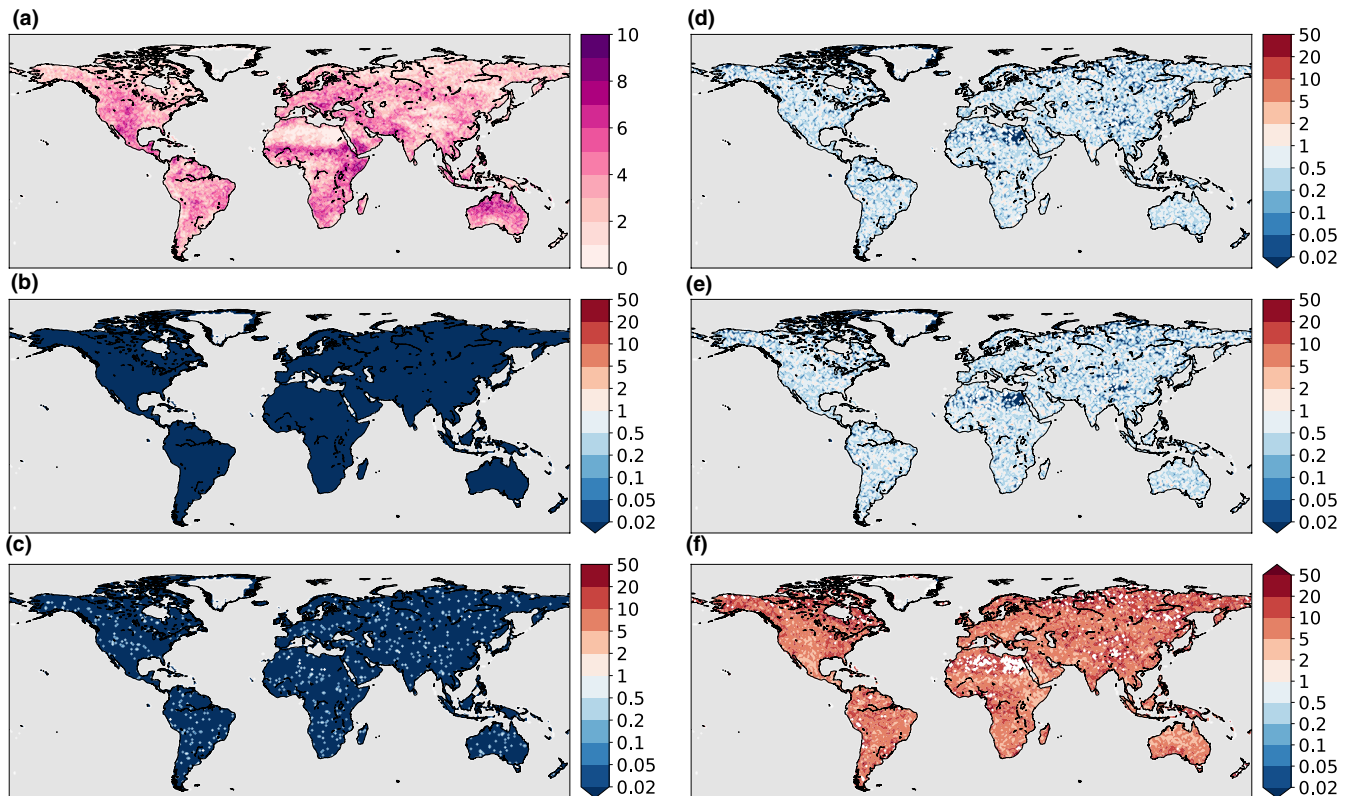


**FIGURE 7** Occurrence of compound extremes. (a) Number of years where temperature exceeds the 90th percentile and precipitation lies below the 10th percentile in the Control scenario. Temperature and precipitation are averaged over the 3 months where vegetation is most active. (b–f) Probability ratio (scenario/control) for the compound hot and dry years (Noextremes (b), Nocompound (c), Hot (d), Dry (e) and Hotdry (f))

of the present-day climate, as well as scenarios with varying intensity and frequency of single and compound drivers. Process-based impact models can then be used to estimate the effects of such varying climate conditions on different types of impacts for different regions.

Here, we present a dataset of daily climate forcing with varying drought-heat signatures for modelling climate impacts. Six 100-year long scenarios cover different conditions, varying from very few extremes overall, over many single drought or heat extremes, to many compound drought and heat events. The scenarios were sampled from a 2,000-year climate dataset representing present-day climate simulated with a global circulation model at  $1^\circ \times 1^\circ$  spatial resolution. Despite differences in the occurrence of droughts and heatwaves between scenarios, their mean climate is comparable and representative of the observed climate of 2011–2015.

The climate forcing was generated with EC-Earth, a fully coupled global climate model (Hazeleger et al., 2012). The 2,000-year climate dataset and its companions with  $+2^\circ\text{C}$  and  $+3^\circ\text{C}$  global climate change has already been used to identify drivers of crop failure (Vogel et al., 2021), study extreme river discharge in a warmer world (Van der Wiel et al., 2019c), evaluate extremes in the renewable energy sector (Van der Wiel et al., 2019a, 2019b), assess changes in heatwaves in India (Nanditha et al., 2020) and detect changes in

mountain-specific climate indicators in a warmer world in High Mountain Asia (Bonekamp et al., 2020), highlighting its applicability for assessing climate impacts.

In addition to temperature and precipitation, we provide a range of variables that are common inputs to climate impact models, including radiation and wind speed (Table 1). Despite a good alignment of global mean temperatures with present-day conditions, EC-Earth is not free of biases at the local to regional scale (Section 2.2). In particular, there is a cold and dry bias in the tropics and a warm and wet bias in the high latitudes (Figure 1). Depending on the application, these biases need to be accounted and potentially be adjusted for when modelling impacts (Vogel et al., 2021). For global vegetation models, a spin-up to equilibrate carbon pools is probably required. Furthermore, given the method presented for the creation of the scenarios, there is no spatial coherence in the dataset, and hence, no correlation in weather conditions between neighbouring locations or around the world. Again, this needs to be taken into account when modelling impacts and precludes modelling impacts for which spatial interactions matter (e.g. many hydrological applications).

The presented scenarios are primarily designed to study the effect of varying drought and heat conditions on terrestrial carbon dynamics. The scenario design, therefore, focuses on creating different likelihoods of dry and/or hot conditions

during the peak of the growing season, when plants are most vulnerable (Section 2). In this context, the scenarios could form the basis for model intercomparison projects (MIPs) using a suite of global vegetation models (Bastos et al., 2020; Friedlingstein et al., 2019; Pan et al., 2020; Zscheischler et al., 2014b). Despite the focus on the carbon cycle during the design of the scenarios, we believe they also could be well-suited for studying the differential effects of droughts and heatwaves on other impact types, for instance with the impact models used in the Inter-Sectoral Impact Model Intercomparison Project (ISIMIP, <https://www.isimip.org>; Warszawski et al., 2014). Two impact types that we deem of particular relevance here are wildfire occurrence and agriculture. Outside hot and dry conditions, factors such as wind speed, lightning occurrence and land-use change govern wildfire risk. Our scenarios could be used to investigate how wildfire regimes change under different drought-heat regimes and may help pin down reasons behind the large differences in modelled fire characteristics across models (Forkel et al., 2019; Teckentrup et al., 2019). Common protocols for modelling wildfire occurrence have already been set up in the FireMIP (Rabin et al., 2017). Note, however, that the effect of spatial interactions cannot be simulated with our scenarios, as there is no spatial coherence. Another possible area of application of the scenarios are crop models, as for instance collected in the Agricultural Model Intercomparison and Improvement Project (AgMIP, <https://agmip.org>, Rosenzweig et al., 2013). AgMIP focuses specifically on agricultural impacts and is designed to study and improve world food security. Crops are highly sensitive to hot and dry conditions (Cohen et al., 2020; Shah & Paulsen, 2003) and crop models differ strongly in their response to climate extremes and climate change (Rosenzweig et al., 2014) though uncertainties have been reduced recently (Toreti et al., 2020). Our scenarios might help to disentangle how different crop models respond to different types of droughts, heatwaves and compound drought and heatwave events.

## AUTHOR CONTRIBUTIONS

J.Z. conceived the study. E.T. performed all analysis, performed model simulations with LPX-Bern, created all figures and wrote the first draft. K.v.d.W. performed the model simulations with EC-Earth. S.L. and F.J. helped with the setup of LPX-Bern and interpretation of the results. All authors contributed substantially to the writing and revisions of the manuscript.

## OPEN PRACTICES

This article has earned an Open Data badge for making publicly available the digitally-shareable data necessary to reproduce the reported results. The data is available at <https://doi.org/10.5281/zenodo.4385445>. Learn more about the Open Practices badges from the Center for OpenScience: <https://osf.io/tyyxz/wiki>.

## ORCID

Elisabeth Tschumi  <https://orcid.org/0000-0001-9062-2396>

## REFERENCES

- Allen, C.D., Macalady, A.K., Chenchouni, H., Bachelet, D., McDowell, N., Vennetier, M. et al. (2010) A global overview of drought and heat-induced tree mortality reveals emerging climate change risks for forests. *Forest Ecology and Management*, 259, 660–684. Available from: <https://doi.org/10.1016/j.foreco.2009.09.001>
- Anderegg, W.R., Kane, J.M. & Anderegg, L.D. (2013) Consequences of widespread tree mortality triggered by drought and temperature stress. *Nature Climate Change*, 3, 30–36.
- Bastos, A., Ciais, P., Friedlingstein, P., Sitch, S., Pongratz, J., Fan, L. et al. (2020) Direct and seasonal legacy effects of the 2018 heat wave and drought on European ecosystem productivity. *Science Advances*, 6, eaba2724. Available from: <https://doi.org/10.1126/sciadv.aba2724>
- Beier, C., Beierkuhnlein, C., Wohlgemuth, T., Penuelas, J., Emmett, B., Körner, C. et al. (2012) Precipitation manipulation experiments – challenges and recommendations for the future. *Ecology Letters*, 15, 899–911.
- Bonekamp, P.N.J., Wanders, N., van der Wiel, K., Lutz, A.F. & Immerzeel, W.W. (2020) Using large ensemble modelling to derive future changes in mountain specific climate indicators in a 2 and 3°C warmer world in High Mountain Asia. *International Journal of Climatology*. Available from: 41(S1), E964–E979. <https://doi.org/10.1002/joc.6742>
- Buizza, R., Milleer, M. & Palmer, T.N. (1999) Stochastic representation of model uncertainties in the ECMWF ensemble prediction system. *Quarterly Journal of the Royal Meteorological Society*, 125, 2887–2908.
- Ciais, P., Reichstein, M., Viovy, N., Granier, A., Ogée, J., Allard, V. et al. (2005) Europe-wide reduction in primary productivity caused by the heat and drought in 2003. *Nature*, 437, 529–533. Available from: <https://doi.org/10.1038/nature03972>
- Cohen, I., Zandalinas, S.I., Huck, C., Fritschi, F.B. & Mittler, R. (2020) Meta-analysis of drought and heat stress combination impact on crop yield and yield components. *Physiologia Plantarum*, 171, 66–76. Available from: <https://doi.org/10.1111/ppl.13203>
- De Boeck, H.J., Dreesen, F.E., Janssens, I.A. & Nijs, I. (2011) Whole-system responses of experimental plant communities to climate extremes imposed in different seasons. *New Phytologist*, 189, 806–817.
- Flach, M., Gans, F., Brenning, A., Denzler, J., Reichstein, M., Rodner, E. et al. (2017) Multivariate anomaly detection for Earth observations: a comparison of algorithms and feature extraction techniques. *Earth System Dynamics*, 8, 677–696. Available from: <https://doi.org/10.5194/esd-8-677-2017>
- Forkel, M., Andela, N., Harrison, S.P., Lasslop, G., van Marle, M., Chuvieco, E. et al. (2019) Emergent relationships with respect to burned area in global satellite observations and fire-enabled vegetation models. *Biogeosciences*, 16, 57–76. Available from: <https://doi.org/10.5194/bg-16-57-2019>
- Frank, D., Reichstein, M., Bahn, M., Thonicke, K., Frank, D., Mahecha, M.D. et al. (2015) Effects of climate extremes on the terrestrial carbon cycle: concepts, processes and potential future impacts. *Global Change Biology*, 21, 2861–2880.
- Friedlingstein, P., Jones, M.W., O'Sullivan, M., Andrew, R.M., Hauck, J., Peters, G.P. et al. (2019) Global carbon budget 2019. *Earth System Science Data*, 11, 1783–1838.

- Friedlingstein, P., Meinshausen, M., Arora, V.K., Jones, C.D., Anav, A., Liddicoat, S.K. et al. (2014) Uncertainties in CMIP5 climate projections due to carbon cycle feedbacks. *Journal of Climate*, 27, 511–526.
- Friedlingstein, P., O'Sullivan, M., Jones, M.W., Andrew, R.M., Hauck, J., Olsen, A. et al. (2020) Global carbon budget 2020. *Earth System Science Data*, 12, 3269–3340. Available from: <https://doi.org/10.5194/essd-12-3269-2020>
- Harris, I., Jones, P.D., Osborn, T.J. & Lister, D.H. (2014) Updated high-resolution grids of monthly climatic observations—the CRU TS3. Dataset, *International Journal of Climatology*, 34, 623–642.
- Hazeleger, W., Wang, X., Severijns, C., Ștefănescu, S., Bintanja, R., Sterl, A. et al. (2012) EC-Earth V2. 2: description and validation of a new seamless earth system prediction model. *Climate Dynamics*, 39, 2611–2629.
- IPCC. (2012) *Managing the risks of extreme events and disasters to advance climate change adaptation: special report of the Intergovernmental Panel on Climate Change*. Cambridge University Press. Available from: <https://doi.org/10.1017/CBO9781139177245>
- Laufkötter, C., Zscheischler, J. & Frölicher T.L. (2020) High-impact marine heatwaves attributable to human-induced global warming. *Science*, 369, 1621–1625. Available from: <https://doi.org/10.1126/science.aba0690>
- Leonard, M., Westra, S., Phatak, A., Lambert, M., van den Hurk, B., McInnes, K. et al. (2014) A compound event framework for understanding extreme impacts. *Wiley Interdisciplinary Reviews: Climate Change*, 5, 113–128.
- Lienert, S. & Joos, F. (2018) A Bayesian ensemble data assimilation to constrain model parameters and land-use carbon emissions. *Biogeosciences*, 15, 2909–2930.
- Madden, R.A. & Williams, J. (1978) The correlation between temperature and precipitation in the United States and Europe. *Monthly Weather Review*, 106, 142–147.
- McKee, T.B., Doesken, N.J. & Kleist, J. (1993) The relationship of drought frequency and duration to time scales. In: *Proceedings of the 8th conference on applied climatology*, vol. 17. Boston, pp. 179–183. American Meteorological Society.
- Nanditha, J., van derWiel, K., Bhatia, U., Stone, D., Selton, F. & Mishra, V. (2020) A seven-fold rise in the probability of exceeding the observed hottest summer in India in a 2°C warmer world. *Environmental Research Letters*, 15, 044028. Available from: <https://doi.org/10.1088/1748-9326/ab7555>
- Orth, R., Zscheischler, J. & Seneviratne, S.I. (2016) Record dry summer in 2015 challenges precipitation projections in Central Europe. *Scientific Reports*, 6, 1–8.
- Pan, S., Yang, J., Tian, H., Shi, H., Chang, J., Ciais, P. et al. (2020) Climate extreme versus carbon extreme: responses of terrestrial carbon fluxes to temperature and precipitation. *Journal of Geophysical Research: Biogeosciences*, 125, e2019JG005252. Available from: <https://doi.org/10.1029/2019JG005252>
- Pastorello, G., Trotta, C., Canfora, E., Chu, H., Christianson, D., Cheah, Y.-W. et al. (2020) The FLUXNET2015 dataset and the ONEFlux processing pipeline for eddy covariance data. *Scientific Data*, 7, 1–27.
- Perkins, S.E. (2015) A review on the scientific understanding of heatwaves—their measurement, driving mechanisms, and changes at the global scale. *Atmospheric Research*, 164, 242–267.
- Rabin, S.S., Melton, J.R., Lasslop, G., Bachelet, D., Forrest, M., Hantson, S. et al. (2017) The Fire Modeling Intercomparison Project (FireMIP), phase 1: experimental and analytical protocols with detailed model descriptions. *Geoscientific Model Development*, 10, 1175–1197.
- Rammig, A., Wiedermann, M., Donges, J.F., Babst, F., von Bloh, W., Frank, D. et al. (2015) Coincidences of climate extremes and anomalous vegetation responses: comparing tree ring patterns to simulated productivity. *Biogeosciences*, 12, 373–385. Available from: <https://doi.org/10.5194/bg-12-373-2015>
- Reichstein, M., Bahn, M., Ciais, P., Frank, D., Mahecha, M.D., Seneviratne, S.I. et al. (2013) Climate extremes and the carbon cycle. *Nature*, 500, 287–295.
- Ribeiro, A.F.S., Russo, A., Gouveia, C.M., Páscoa, P. & Zscheischler, J. (2020) Risk of crop failure due to compound dry and hot extremes estimated with nested copulas. *Biogeosciences*, 17, 4815–4830.
- Rosenzweig, C., Elliott, J., Deryng, D., Ruane, A.C., Müller, C., Arneth, A. et al. (2014) Assessing agricultural risks of climate change in the 21st century in a global gridded crop model intercomparison. *Proceedings of the National Academy of Sciences of the United States of America*, 111, 3268–3273. Available from: <https://doi.org/10.1073/pnas.1222463110>
- Rosenzweig, C., Jones, J.W., Hatfield, J.L., Ruane, A.C., Boote, K.J., Thorburn, P. et al. (2013) The agricultural model intercomparison and improvement project (AgMIP): protocols and pilot studies. *Agricultural and Forest Meteorology*, 170, 166–182.
- Schlesinger, W.H. & Bernhard, E.S. (2013) *Biogeochemistry: an analysis of global change*, 3rd edition, San Diego: Academic Press/Elsevier.
- Seneviratne, S.I., Nicholls, N., Easterling, D., Goodess, C., Kanae, S., Kossin, J. et al. (2012) Changes in climate extremes and their impacts on the natural physical environment. In: Field, C., Barros, V., Stocker, T., Qin, D., Dokken, D., Ebi, K., Mastrandrea, M., Mach, K., Plattner, G.-K., Allen, S., Tignor, M. & Midgley, P. (Eds.) *Managing the risks of extreme events and disasters to advance climate change adaptation*. Cambridge and New York, NY: Cambridge University Press, pp. 109–230.
- Shah, N. & Paulsen, G. (2003) Interaction of drought and high temperature on photosynthesis and grain-filling of wheat. *Plant and Soil*, 257, 219–226.
- Sippel, S., Reichstein, M., Ma, X., Mahecha, M.D., Lange, H., Flach, M. et al. (2018) Drought, heat, and the carbon cycle: a review. *Current Climate Change Reports*, 4, 266–286.
- Sitch, S., Huntingford, C., Gedney, N., Levy, P., Lomas, M., Piao, S. et al. (2008) Evaluation of the terrestrial carbon cycle, future plant geography and climate-carbon cycle feedbacks using five Dynamic Global Vegetation Models (DGVMs). *Global Change Biology*, 14, 2015–2039.
- Song, J., Wan, S., Piao, S., Knapp, A.K., Classen, A.T., Vicca, S. et al. (2019) A meta-analysis of 1,119 manipulative experiments on terrestrial carbon-cycling responses to global change. *Nature Ecology & Evolution*, 3, 1309–1320. Available from: <https://doi.org/10.1038/s41559-019-0958-3>
- Stocker, B.D., Zscheischler, J., Keenan, T.F., Prentice, I.C., Seneviratne, S.I. & Peñuelas, J. (2019) Drought impacts on terrestrial primary production underestimated by satellite monitoring. *Nature Geoscience*, 12, 264–270.
- Sun, Q., Miao, C., Duan, Q., Ashouri, H., Sorooshian, S. & Hsu, K.-L. (2018) A review of global precipitation data sets: data sources, estimation, and intercomparisons. *Reviews of Geophysics*, 56, 79–107.
- Taylor, K.E., Stouffer, R.J. & Meehl, G.A. (2012) An overview of CMIP5 and the experiment design. *Bulletin of the American Meteorological Society*, 93, 485–498. Available from: <https://doi.org/10.1175/BAMS-D-11-00094.1>
- Teckentrup, L., Harrison, S.P., Hantson, S., Heil, A., Melton, J.R., Forrest, M. et al. (2019) Response of simulated burned area to historical changes in environmental and anthropogenic factors: a comparison of seven fire models. *Biogeosciences*, 16, 3883–3910. Available from: <https://doi.org/10.5194/bg-16-3883-2019>

- Tian, H., Yang, J., Lu, C., Xu, R., Canadell, J.G., Jackson, R.B. et al. (2018) The global N<sub>2</sub>O model intercomparison project. *Bulletin of the American Meteorological Society*, 99, 1231–1251.
- Toreti, A., Deryng, D., Tubiello, F.N., Müller, C., Kimball, B.A., Moser, G. et al. (2020) Narrowing uncertainties in the effects of elevated CO<sub>2</sub> on crops. *Nature Food*, 1, 775–782. Available from: <https://doi.org/10.1038/s43016-020-00195-4>
- Trenberth, K.E. & Shea, D.J. (2005) Relationships between precipitation and surface temperature. *Geophysical Research Letters*, 32(14), L14703.
- Tschumi, E., Lienert, S., van der Wiel, K., Joos, F. & Zscheischler, J. (2020) A climate database with varying drought-heat signatures for climate impact modelling. Available from: <https://doi.org/10.5281/zenodo.4385445>
- Tschumi, E. & Zscheischler, J. (2020) Countrywide climate features during recorded climate-related disasters. *Climatic Change*, 158, 593–609. Available from: <https://doi.org/10.1007/s10584-019-02556-w>
- Van der Wiel, K., Bloomfield, H.C., Lee, R.W., Stoop, L.P., Blackport, R., Screen, J.A. et al. (2019a) The influence of weather regimes on European renewable energy production and demand. *Environmental Research Letters*, 14, 094010. Available from: <https://doi.org/10.1088/1748-9326/ab38d3>
- Van der Wiel, K., Selten, F.M., Bintanja, R., Blackport, R. & Screen, J.A. (2020) Ensemble climate-impact modelling: extreme impacts from moderate meteorological conditions. *Environmental Research Letters*, 15, 034050.
- Van der Wiel, K., Stoop, L.P., Van Zuijlen, B., Blackport, R., Van den Broek, M. & Selten, F. (2019b) Meteorological conditions leading to extreme low variable renewable energy production and extreme high energy shortfall. *Renewable and Sustainable Energy Reviews*, 111, 261–275. <https://doi.org/10.1016/j.rser.2019.04.065>
- Van der Wiel, K., Wanders, N., Selten, F. & Bierkens, M. (2019c) Added value of large ensemble simulations for assessing extreme river discharge in a 2 C warmer world. *Geophysical Research Letters*, 46, 2093–2102.
- Vicente-Serrano, S.M., Beguería, S. & López-Moreno, J.I. (2010) A multi-scalar drought index sensitive to global warming: the standardized precipitation evapotranspiration index. *Journal of Climate*, 23, 1696–1718.
- Vogel, J., Rivoire, P., Deidda, C., Rahimi, L., Sauter, C.A., Tschumi, E., van der Wiel, K., Zhang, T. & Zscheischler, J. (2021) Identifying meteorological drivers of extreme impacts: an application to simulated crop yields. *Earth System Dynamics*, 12, 151–172. <https://doi.org/10.5194/esd-12-151-2021>
- von Buttlar, J., Zscheischler, J., Rammig, A., Sippel, S., Reichstein, M., Knohl, A. et al. (2018) Impacts of droughts and extreme-temperature events on gross primary production and ecosystem respiration: a systematic assessment across ecosystems and climate zones. *Biogeosciences*, 15, 1293–1318.
- Wang, B. & Ding, Q. (2008) Global monsoon: dominant mode of annual variation in the tropics. *Dynamics of Atmospheres and Oceans*, 44, 165–183.
- Warszawski, L., Frieler, K., Huber, V., Piontek, F., Serdeczny, O. & Schewe, J. (2014) The inter-sectoral impact model intercomparison project (ISI-MIP): project framework. *Proceedings of the National Academy of Sciences of the United States of America*, 111, 3228–3232.
- Wieder, W., Boehner, J., Bonan, G. & Langseth, M. (2014) *Regridded harmonized world soil database v1. 2*. Oak Ridge, Tennessee, USA: ORNL DAAC.
- Xu, C., McDowell, N.G., Fisher, R.A., Wei, L., Sevanto, S., Christoffersen, B.O. et al. (2019) Increasing impacts of extreme droughts on vegetation productivity under climate change. *Nature Climate Change*, 9, 948–953.
- Zhao, M. & Running, S.W. (2010) Drought-induced reduction in global terrestrial net primary production from 2000 through 2009. *Science*, 329, 940–943. Available from: <https://doi.org/10.1126/science.1192666>
- Zhu, Z., Piao, S., Myneni, R.B., Huang, M., Zeng, Z., Canadell, J.G. et al. (2016) Greening of the Earth and its drivers. *Nature Climate Change*, 6, 791–795.
- Zscheischler, J., Fatichi, S., Wolf, S., Blanken, P.D., Bohrer, G., Clark, K. et al. (2016) Short-term favorable weather conditions are an important control of interannual variability in carbon and water fluxes. *Journal of Geophysical Research: Biogeosciences*, 121, 2186–2198.
- Zscheischler, J., Mahecha, M.D., Harmeling, S. & Reichstein, M. (2013) Detection and attribution of large spatiotemporal extreme events in Earth observation data. *Ecological Informatics*, 15, 66–73. Available from: <https://doi.org/10.1016/j.ecoinf.2013.03.004>
- Zscheischler, J., Mahecha, M.D., Von Buttlar, J., Harmeling, S., Jung, M., Rammig, A. et al. (2014a) A few extreme events dominate global interannual variability in gross primary production. *Environmental Research Letters*, 9, 035001. Available from: <https://doi.org/10.1088/1748-9326/9/3/035001>
- Zscheischler, J., Martius, O., Westra, S., Bevacqua, E., Raymond, C., Horton, R.M. et al. (2020) A typology of compound weather and climate events. *Nature Reviews Earth and Environment*, 1, 333–347. Available from: <https://doi.org/10.1038/s43017-020-0060-z>
- Zscheischler, J., Michalak, A.M., Schwalm, C., Mahecha, M.D., Huntzinger, D.N., Reichstein, M. et al. (2014b) Impact of large-scale climate extremes on biospheric carbon fluxes: an intercomparison based on MsTMIP data. *Global Biogeochemical Cycles*, 28, 585–600. Available from: <https://doi.org/10.1002/2014GB004826>
- Zscheischler, J., Orth, R. & Seneviratne, S.I. (2017) Bivariate return periods of temperature and precipitation explain a large fraction of European crop yields. *Biogeosciences*, 14, 3309–3320. Available from: <https://doi.org/10.5194/bg-14-3309-2017>
- Zscheischler, J., Reichstein, M., Harmeling, S., Rammig, A., Tomelleri, E. & Mahecha, M.D. (2014c) Extreme events in gross primary production: a characterization across continents. *Biogeosciences*, 11, 2909–2924. Available from: <https://doi.org/10.5194/bg-11-2909-2014>
- Zscheischler, J., Reichstein, M., Von Buttlar, J., Mu, M., Randerson, J.T. & Mahecha, M.D. (2014d) Carbon cycle extremes during the 21<sup>st</sup> century in CMIP5 models: future evolution and attribution to climatic drivers. *Geophysical Research Letters*, 41, 8853–8861.
- Zscheischler, J. & Seneviratne, S.I. (2017) Dependence of drivers affects risks associated with compound events. *Science Advances*, 3, e1700263. Available from: <https://doi.org/10.1126/sciadv.1700263>
- Zscheischler, J., Westra, S., Van Den Hurk, B.J., Seneviratne, S.I., Ward, P.J., Pitman, A. et al. (2018) Future climate risk from compound events. *Nature Climate Change*, 8, 469–477.

## SUPPORTING INFORMATION

Additional supporting information may be found online in the Supporting Information section.

**How to cite this article:** Tschumi, E., Lienert, S., van der Wiel, K., Joos, F. & Zscheischler, J. (2021) A climate database with varying drought-heat signatures for climate impact modelling. *Geoscience Data Journal*, 00, 1–13. <https://doi.org/10.1002/gdj3.129>